Electronic Supplementary Information

Discrimination between two memory channels by molecular alloying in a doubly bistable spin crossover material

Francisco Javier Valverde-Muñoz, Maksym Seredyuk, Manuel Meneses-Sanchez, M. Carmen Muñoz, Carlos Bartual-Murgui, José A. Real

Table S1. Crystallographic parameters for **100As**, **71As** and **100Ni**.

	100As		**71As**			**100Ni**
T (K)	230 K	300 K	230 K	120 K (quenched)	157 K	110 K
Empirical formula	$C_{30}H_{48}As_2F_{12}FeN_{10}$		$C_{30}H_{48}As_{1.42}F_{12}FeN_{10}P_{0.58}$			$C_{30}H_{48}F_{12}N_{10}NiP_2$
Mr	982.47		956.98			897.43
Crystal system	triclinic		triclinic			triclinic
Space group	$P\bar{1}$		$P\bar{1}$			$P\bar{1}$
a (Å)	9.4189(8)	9.6140(7)	9.411(3)	9.2858(5)	9.588(3)	9.1245 (3)
b (Å)	10.3506(9)	10.2571(6)	10.309(3)	10.4090(6)	10.065(2)	10.5150 (2)
c (Å)	22.444(2)	21.9999(13)	22.379(5)	22.272(2)	21.074(4)	21.6376 (4)
α	91.428(7)	91.522(5)	91.520(11)	83.796(5)	93.89(2)	83.769 (2)
β	100.894(7)	96.193(6)	100.995(12)	78.275(5)	93.68(2)	78.852 (2)
γ	99.001(7)	98.456(6)	98.955(16)	81.416(5)	100.47(2)	81.928 (2)
V (Å^3)	2118.8(3)	2131.3(2)	2101.8(11)	2077.5(2)	1989.2(8)	2009.56 (9)
Z	2		2			2
F(000)	996	996	976.0	975	975	928
D_c (mg cm^{-3})	1.540	1.531	1.514	1.530	1.598	1.483
μ (Mo-K_α)(mm^{-1})	1.993	1.982	1.597	1.597	1.668	
No. of total reflections						
[$I>2\sigma(I)$]	5545	3523	10380	4016	2958	6677
R [$I>2\sigma(I)$]	0.0646	0.0903	0.0563	0.0516	0.1247	0.042
wR [$I>2\sigma(I)$]	0.1470	0.2341	0.1406	0.0969	0.2859	0.131
S	1.013	0.946	1.050	1.047	1.008	0.72

Table S2. Selected bond lengths (Å) and angles (°)for **100As** at indicated temperatures.

	100As		**71As**		
	230 K (**HS**[1])	300 K (**HS**[2])	120 K (**HS**[1]+**LS**[1])	157 K (**LS**[2])	230 K (**HS**[2])
Fe-N1	2.228(4)	2.219(7)	2.206(5)	1.962(11)	2.222(3)
Fe-N2	2.184(4)	2.185(6)	2.164(4)	1.969(10)	2.181(3)
Fe-N3	2.214(4)	2.212(6)	2.204(4)	1.967(10)	2.215(3)
Fe-N4	2.194(4)	2.173(7)	2.194(5)	1.948(11)	2.196(3)
Fe-N5	2.174(4)	2.165(6)	2.154(3)	1.959(10)	2.173(3)
Fe-N6	2.198(4)	2.169(7)	2.190(4)	1.980(9)	2.192(3)
<Fe–N>	2.199	2.187	2.185	1.964	2.197
N1-Fe-N2	75.0(2)	74.9(2)	75.4(2)	80.6(4)	74.99(10)
N1-Fe-N3	92.9(2)	91.6(2)	93.8(2)	93.0(4)	92.64(11)
N1-Fe-N4	167.6(2)	166.4(3)	168.9(2)	173.8(4)	167.34(11)
N1-Fe-N5	84.4(2)	85.2(2)	84.5(2)	91.4(4)	84.38(11)
N1-Fe-N6	88.2(2)	88.9(2)	87.8(2)	89.1(4)	88.57(11)
N2-Fe-N3	98.2(2)	97.8(2)	97.60(14)	92.1(4)	98.22(11)
N2-Fe-N4	102.5(2)	103.4(2)	102.4(2)	96.0(4)	102.73(11)
N2-Fe-N5	158.4(2)	159.7(2)	159.0(2)	171.8(4)	158.30(11)
N2-Fe-N6	97.1(2)	99.5(2)	97.19(14)	96.6(4)	96.78(11)
N3-Fe-N4	75.3(2)	75.2(2)	75.6(2)	81.9(4)	75.24(10)
N3-Fe-N5	89.2(2)	86.7(2)	89.49(14)	90.3(4)	89.26(11)
N3-Fe-N6	164.4(2)	162.1(2)	165.05(13)	171.3(4)	164.74(11)
N4-Fe-N5	99.0(2)	97.0(2)	98.4(2)	92.1(4)	98.87(11)
N4-Fe-N6	104.3(2)	104.7(3)	103.3(2)	96.5(4)	104.08(10)
N5-Fe-N6	75.4(2)	75.5(3)	75.85(14)	81.3(4)	75.72(11)

Table S3. Selected bond lengths (Å) and angles (°) for **100Ni** at 110 K.

	100Ni
Ni-N1	2.100(2)
Ni-N2	2.119(2)
Ni-N3	2.098(2)
Ni-N4	2.131(2)
Ni-N5	2.064(2)
Ni-N6	2.147(2)
<Fe–N>	2.110
N1-Ni-N2	78.43(6)
N1-Ni-N4	172.44(6)
N1-Ni-N6	88.44(6)
N2-Ni-N4	96.71(6)
N2-Ni-N6	94.45(6)
N3-Ni-N1	95.96(6)
N3-Ni-N2	95.34(6)
N3-Ni-N4	78.62(6)
N3-Ni-N6	169.90(6)
N4-Ni-N6	97.76(6)
N5-Ni-N1	89.36(6)
N5-Ni-N2	166.24(6)
N5-Ni-N3	92.20(7)
N5-Ni-N4	96.06(6)
N5-Ni-N6	78.72(6)

Table S4. Percentage of intermolecular contacts and void space obtained from the Hirshfeld surface[1] for **100P** and **100As** at 230 K (**HS[1]**) and **100As** at 300 K (**HS[2]**).

Intermolecular contact	**100P** (**HS[1]**, 150 K)	**100As** (**HS[1]**, 230 K)	**100As** (**HS[2]**, 300 K)
C···F (%)	0.7	1.4	0.9
F···H (%)	31.9	33.1	34.1
N···H (%)	3.7	3.1	1.7
C···H (%)	6.4	8.2	3.0
Void space/Å^3 [a,2]	46.54	43.83	27.10
Unit cell volume/Å^3	2076.46	2118.8	2131.3
% void space[b]	2.24	2.07	1.27

[a] Isovalue 0.0003 e AU^3; [b] Referred to unit cell volume.

[1]M. J. Turner, J. J. McKinnon, S. K. Wolff, D. J. Grimwood, P. R. Spackman, D. Jayatilaka and M. A. Spackman, CrystalExplorer17 (2017). University of Western Australia. http://hirshfeldsurface.ne

[2]M. J. Turner, J. J. McKinnon, D. Jayatilaka, M. A. Spackman, *CrystEngComm*, 2011, 13, 1804-1813.

Figure S1. Dependence of $\chi_M T$ vs T on the scan rate.

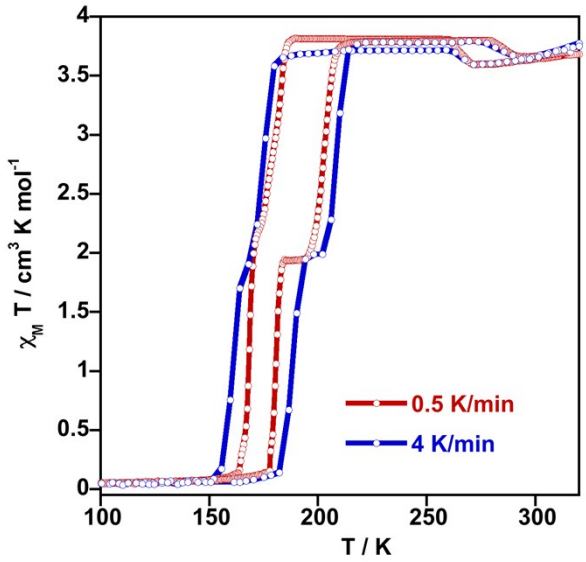

Figure S2. Dependence of $\chi_M T$ vs T on the scan rate.

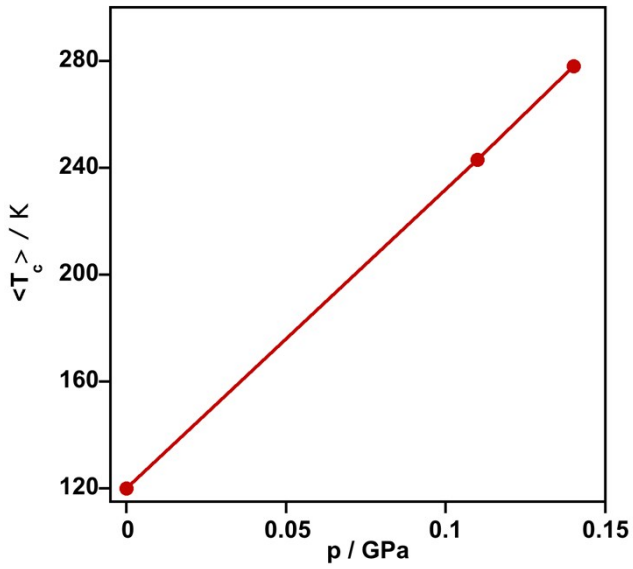

Figure S3. Temperature dependence of $\chi_M T$ vs T for the molecular alloys **86As, 63As and 12As** (scan rate 2 K min^{-1}).

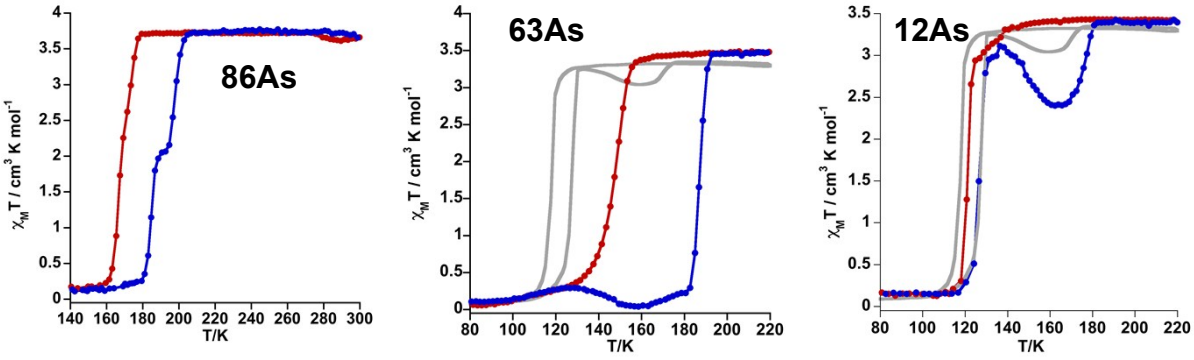

Figure S4. Dependence of the hysteretic behavior of the **HS^1↔HS^2** structural phase transition on the concentration of three selected samples (100As, 71As and 56As).

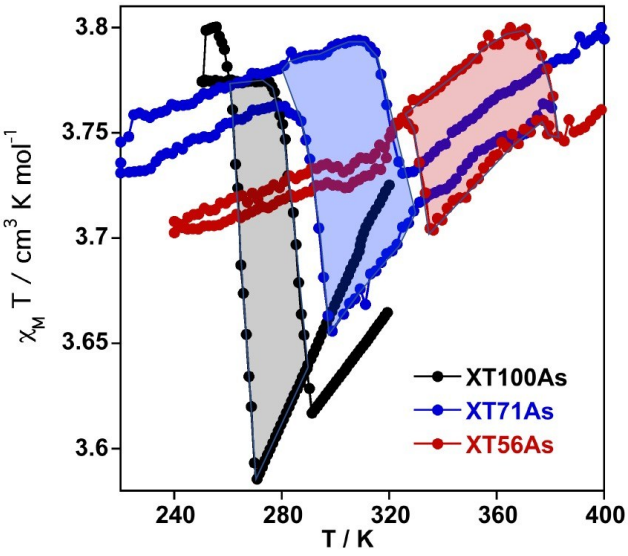

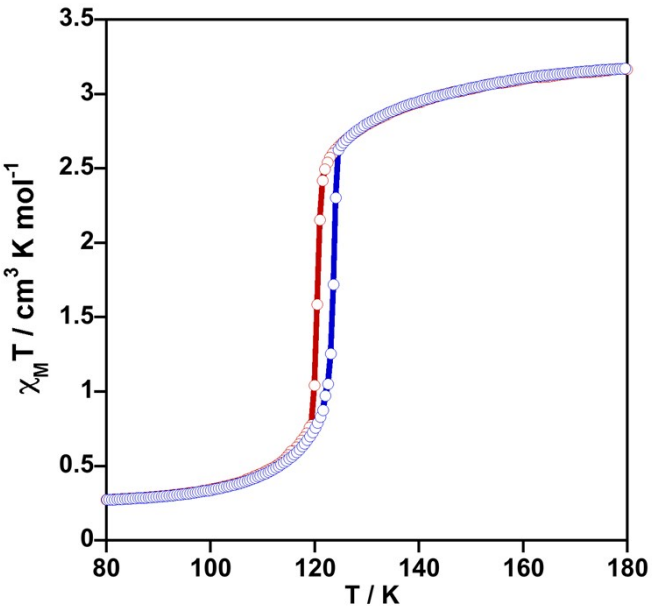

Figure S5. Temperature dependence of $\chi_M T$ vs T for **17Ni**.

Figure S6. Temperature dependence of $\chi_M T$ vs T for **100Ni**.

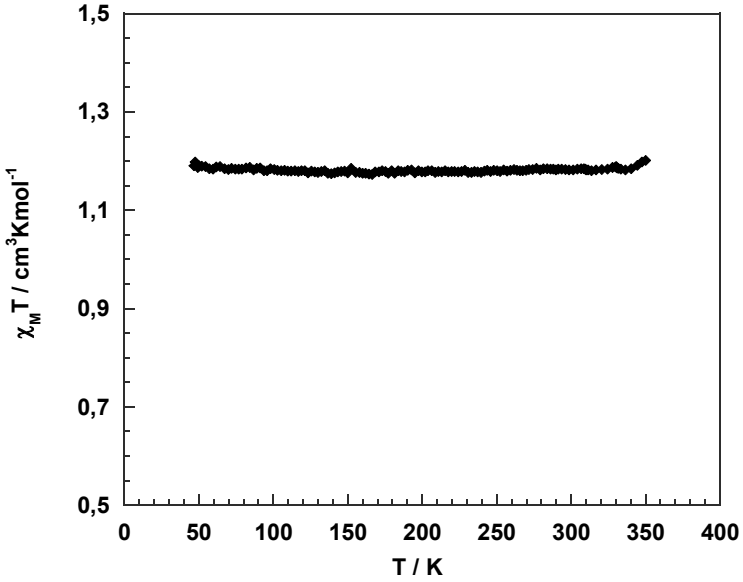
1,5
1,3
1,1
0,9
0,7
0,5
$\chi_M T$ / $cm^3 K mol^{-1}$
0
50
100
150
200
250
300
350
400
T / K

Figure S7. Comparison of cation $[Fe(n\text{Bu-im})_3(tren)]^{2+}$, illustrating larger disorder or butyl groups in **LS²** and **HS²** phases in comparison with **LS¹** and **HS¹**, respectively. Brighter color as well as larger size of thermal ellipsoids shown at 50 % probability corresponds to larger disorder.

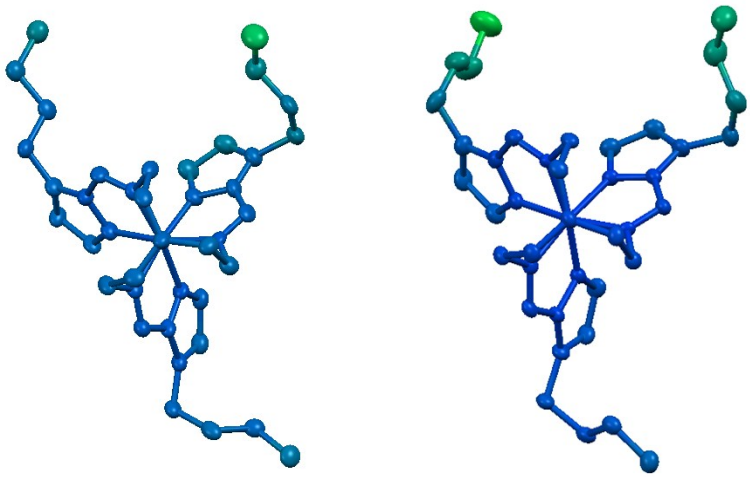

LS¹ **LS²**

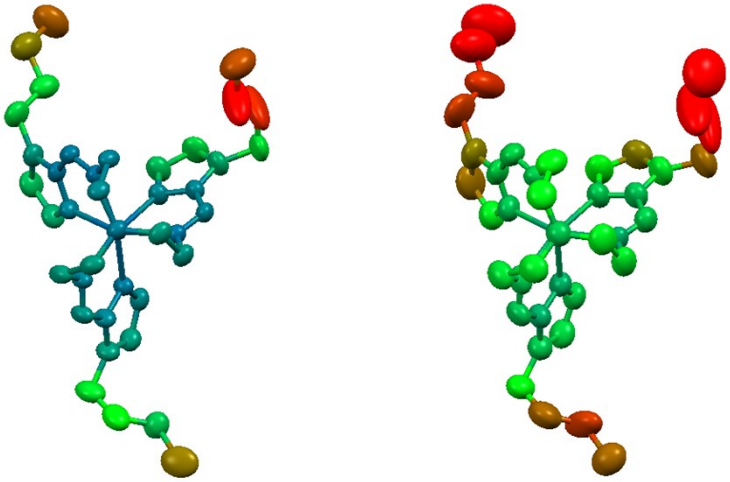

HS¹ **HS²**

Figure S8. (a) Projection of the cation and two anions of **100Ni** with atom numbering scheme. Displacement ellipsoids are shown at the 50% probability level. Hydrogen atoms are omitted for clarity. (b) Overlay of the unit cells for **100P** in **LS**[1] phase (grey bonds) and **100Ni** (red bonds and atoms), both structures at 110 K.

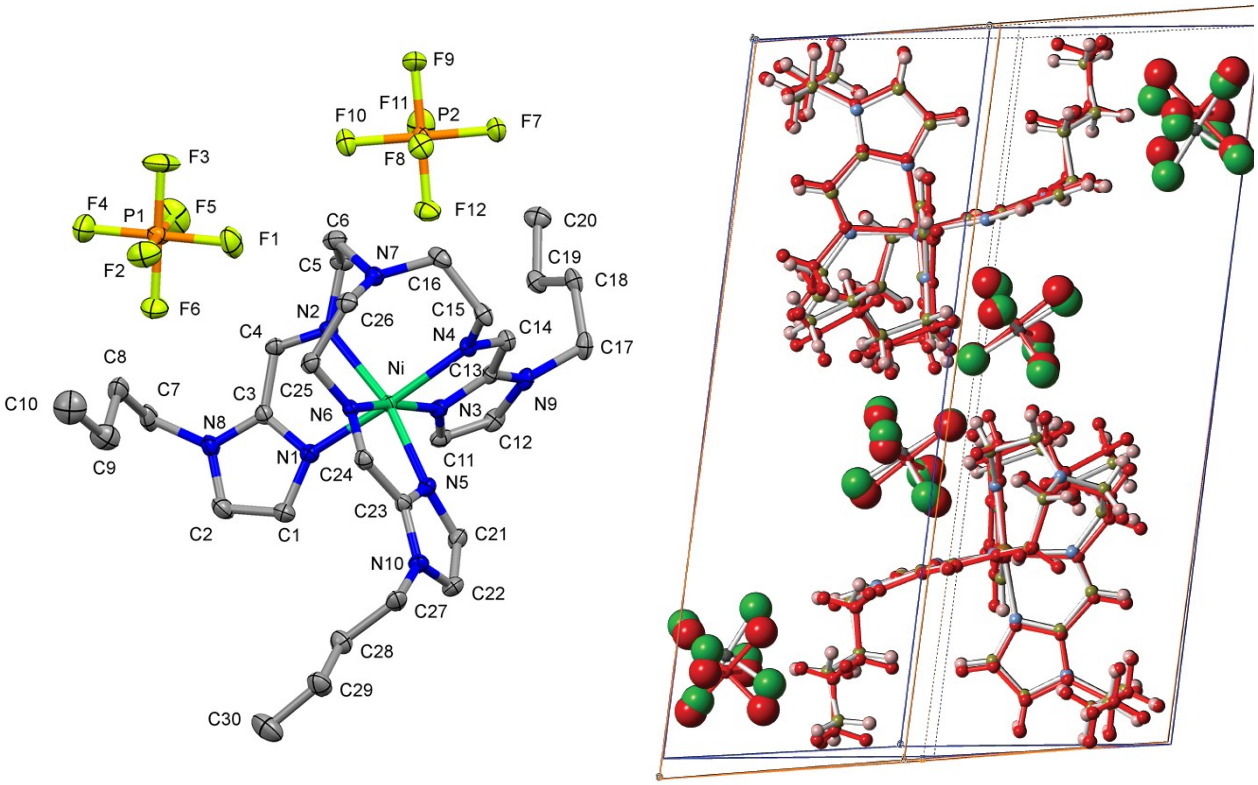

(a) (b)

Figure S9. The Hirshfeld surface mapped with d_{norm} for the complex cation $[Fe(n\text{Bu-im})_3(tren)]^{2+}$ (top) and unit cell voids (bottom) for indicated phases

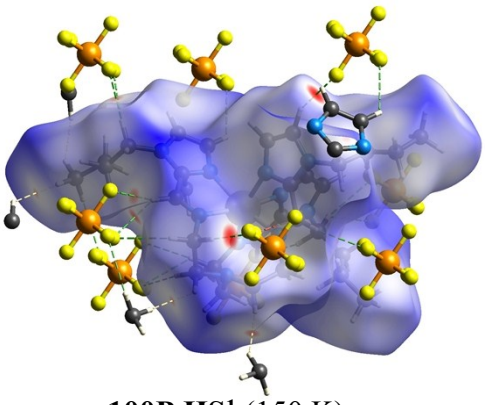

100P HS[1] (150 K)

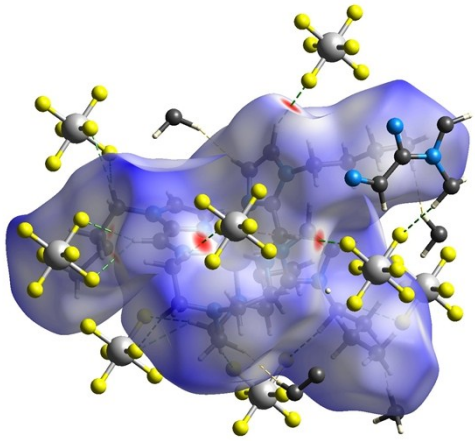

100As HS[1] (230 K)

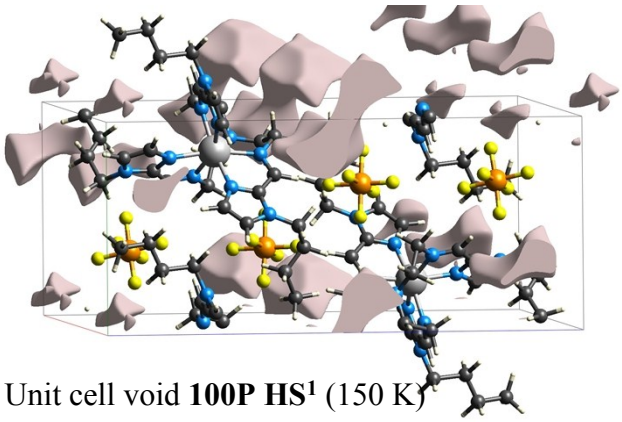

Unit cell void **100P HS[1]** (150 K)

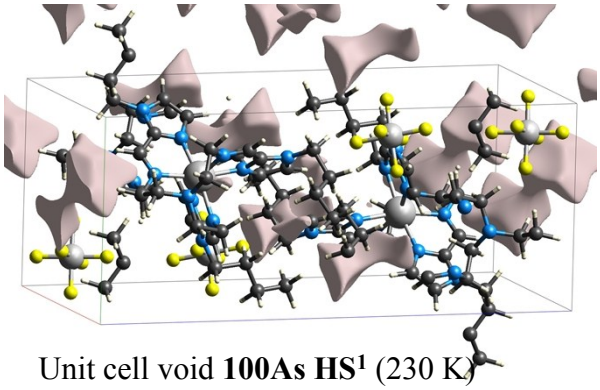

Unit cell void **100As HS[1]** (230 K)

Figure S10. Infra-red spectra of representative $[Fe(n\text{Bu-im})_3(tren)](P_{1-y}As_yF_6)_2$ molecular alloys